An Ab Initio Study of the Excited States, Isomerization Energy Profiles and Conical Intersections of a Chiral Cyclohexylidene Derivative

Marko Schreiber,[†] Mario Barbatti,*[,‡] Shmuel Zilberg,[§] Hans Lischka,[‡] and Leticia González*[,†]

Institut für Chemie und Biochemie, Freie Universität Berlin, Takustrasse 3, 14195 Berlin, Germany, Institute for Theoretical Chemistry, University of Vienna, Währingerstrasse 17, 1090, Vienna, Austria, Department of Physical Chemistry and the Farkas Center for Light Induced Processes, The Hebrew University of Jerusalem, 91904 Jerusalem, Israel

Received: September 18, 2006; In Final Form: November 20, 2006

The excited valence and Rydberg states of the chiral (4-methylcyclohexylidene) fluoromethane (4MCF) have been investigated using multiconfigurational CASSCF and CASPT2, and coupled-cluster methods (RI-CC2). A 3s Rydberg state is predicted below the valence $^1\pi\pi^*$ state. To gain insight into the photophysics of the cis−trans isomerization of this olefin, potential energy profiles for the valence $^1\pi\pi^*$ state along the twisting and pyramidalization reaction coordinates have been computed using variational methods (CASSCF and multireference configuration interaction with singles and doubles (MR−CISD)). Starting from geometries with energies close to degeneracy in the valence and ground-state curves, three minima on the crossing seam that can be correlated with the conical intersections known for fluoroethylene, have been found. On the basis of these features, the photochemistry of 4MCF is discussed.

1. Introduction

Chiral photostable molecules are an attractive family of photochromic compounds that can be used for chiroptical devices.[1] Certain olefins, like the one presented here, offer switchable states that are spatial mirror images of each other; i.e., they correspond to axial enantiomers, which for simplicity will be addressed as left- and right-handed forms. Chirality is an intriguing phenomenon that not only can be exploited in the design of novel photonic materials[2] but also controls many biological processes, such as molecular recognition, information processing, and DNA replication.[3]

Interestingly, the key switching reaction connecting left- and right-handed forms in some of the chiroptical switches commonly suggested in the literature[4] is a cis−trans isomerization around a carbon double bond. This motif is commonly present in other biological switches, for instance in the chromophore of biological sensors, such as phytochromes,[5] rhodopsin,[6] or the photoactive yellow protein,[7] to name a few. Ethylene is one of the smallest compounds where this process can be studied, and as a consequence, an extensive number of experimental and theoretical publications exist that are dedicated to the understanding of its photochemistry in detail.[8]

Modeling of photochemistry starts with the characterization of the vertical electronic spectrum and is followed by the location of stationary points of the potential energy surfaces (PES), which may be relevant to explain the photoisomerization mechanism. Even more importantly, conical intersections between PES of the same multiplicity are of interest because they allow ultrafast radiationless channels between two electronic states.[9]

The use of quantum chemical methods to describe quantitatively and qualitatively the electronic excited states of ethylene and its derivatives is a continuous challenge due to the valence and Rydberg spectral bands originated from singlet−singlet transitions.[10] The electronic spectrum of ethylene is dominated by an intense band ascribed to the first $^1\pi\pi^*$ valence state (V state), followed by a number of Rydberg series. The zwitterionic state Z ($^1\pi^{*2}$) is a dark state and lies much higher in energy. The spectrum of ethylene derivatives is similar, but with slightly different ordering of the states.[11] The photochemistry of ethylene is based on the presence of several conical intersections between the N, V and Z states. The main channel for V → N internal conversion is controlled by the twist around the double bond concerted with pyramidalization of one of the carbon atoms and hydrogen migration.[12,13] In the case of polar ethylene derivatives, the polarity introduced by the atomic substitution makes these systems reach the region of S_1/S_0 crossing by a simple torsional motion.[14,15]

The chromophore in the cyclohexylidene 4-MeC_6H_9CHF (4MCF) is the C=C double bond. For this reason these systems are expected to have a related photochemistry, as discussed in the preceding paragraph. Until now, however, only the UV spectra of this and other related compounds have been experimentally studied in detail.[16] As shown in ref 16, the Rydberg band N → 3s of 4MCF is found to lie below the V state, which precedes the N → 3p manifold. The replacement of one vinyl hydrogen and one of the hydrogen atoms in the 4-position of the cyclohexane ring makes the system chiral, as is the case of 4MCF with a methyl in the 4-position and a fluorine atom in the vinyl position. Accordingly, circular dichroism (CD) spectra have also been measured, observing opposite signs for the CD signals of the $\pi \rightarrow$ 3s and the $\pi \rightarrow \pi^*$ states.[16] The sign of the $\pi \rightarrow \pi^*$ transition is explained by the substituent effect at the olefin carbon. To the best of our knowledge, the only attempt to describe theoretically the vertical excitation of 4MCF or related systems has been done by one of the authors (L.G.) using time-dependent density functional theory (TD-DFT).[17] However, as described in ref 17, even if TD-DFT reproduces reasonably

* Corresponding authors. E-mail: L.G., leti@chemie.fu-berlin.de; M.B., mario.barbatti@univie.ac.at.
[†] Freie Universität Berlin.
[‡] University of Vienna.
[§] The Hebrew University of Jerusalem.

10.1021/jp066090x CCC: $37.00
Published on Web 12/21/2006

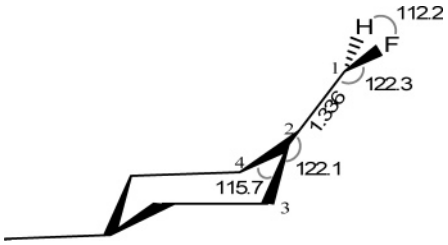

Figure 1. Schematic representation of 4MCF. Bond distances in Å and bond angles in degrees. Adapted from ref 17.

the experimental excitation energies for the two lowest excited states, it predicts a mixture of the $\pi \rightarrow 3s$ and the $\pi \rightarrow \pi^*$ states at the equilibrium geometry, indicating once more that often DFT can give the right answer for the wrong reason.[18] The TD-DFT calculations also pointed to the possibility of having a conical intersection in the vicinity of the twisted structure,[17,19] although the biradical character of the twisted conformation cannot be correctly described within DFT.

Our continuous interest in chiroptical devices,[17,19,20] which could also be controllable through conical intersections, has motivated us to undertake a more extended study of 4MCF, in which the electronically excited states for planar and twisted conformations are properly described by multiconfigurational methods and conical intersections can also be identified reliably. The present work represents the first steps toward the control of the cis−trans isomerization of model chiral olefins like 4MCF. This paper focuses on describing the vertical excitation spectrum by identifying valence and Rydberg states and on locating conical intersections that may be involved in the photoisomerization reaction. Additionally, exploratory potential energy profiles along twisting and pyramidalization coordinates are calculated and the photochemistry of 4MCF is discussed in light of the better understood photoisomerization of fluoroethylene (C_2H_3F), the chromophore of 4MCF.

2. Computational Details

To predict the vertical electronically excited states, two different methodologies have been employed: (a) the state-average multiconfigurational self-consistent field[21] (SA-CASSCF) supplemented with second-order perturbation theory in its multistate version[22] (MS-CASPT2) and (b) the resolution of the identity coupled-cluster with single and doubles[23,24] (RI-CC2).

The vertical-excitation energy calculations have been performed on the ground-state structure optimized at the MP2/6-311+G(d,p) level of theory[17] as implemented in the Gaussian 98 set of programs.[25] The main geometrical parameters (in angstroms and degrees) are given in Figure 1.

The CASSCF/CASPT2 calculations have been performed using two different basis sets: ANO-L 3s2p1d/2s1p (DZ) and ANO-L 4s3p2d/3s2p (TZ+d); the latter one was augmented in the olefin C atoms with a set of extra 1s1p diffuse functions with exponents generated following the standard procedure devised by Kaufman et al.[26] The small basis set has been chosen so as to exclude Rydberg orbitals from the calculation in an approximate way. Accordingly, the active space for the CASSCF calculation using this basis set includes just two electrons in the π and π^* orbitals CAS(2,2) giving rise to three configurations, namely those describing the N, V and Z states. Thus, three states are calculated in a state-averaged way with equal weights, and this will be referred to as SA-3-CAS(2,2)/DZ calculations. In the case of the large basis set, the active space is (2,11), consisting of the two π-orbitals and the 3s, three 3p and five 3d Rydberg orbitals. Twelve states were included in the state-averaging procedure including the N, V, Z and nine Rydberg states with equal weights; thus this level will be referred as SA-12-CAS(2,11)/TZ+d. The active space has been successively increased from (2,2) and decreased from restricted active space SCF[27] [RASSCF(20,20)] including singles and doubles, to get an idea of the influence of the different active spaces on the results.

Single-state (SS) and multi-state (MS) CASPT2 calculations were performed with both active spaces. To avoid the effect of intruder states, a level shift[28] of 0.2 au was necessary in the MS-CASPT2 calculations. This level shift leads to a relative weight of the SA-CASSCF reference wave function in the first-order wave function of about 71%—other states are between 67 and 72%. Transition dipole moments are computed using the CAS state interaction method. The CASPT2 calculations have been performed using the MOLCAS 6.2 set of programs.[29]

To compute properties, the perturbatively modified CASSCF wave function of the MS-CASPT2 treatment has been employed: electric transition dipole moments together with MS-CASPT2 energies were used to calculate oscillator strengths f and rotatory strengths R. The oscillator strength f quantifies the linear charge displacement as a consequence of electronic excitation, but the rotatory strength R is a measure of angular charge displacement associated with the excitation of a chiral molecule. In practice, rotatory strengths can be computed in the so-called dipole length formalism, R^r, using the scalar product of the electric and magnetic transition dipole moments; these values are not origin independent. As an alternative expression the dipole velocity formalism R^v can be employed, which uses the momentum operator to compute electric transition moments. This formalism is origin-independent but has the disadvantage that accurate excitation energies are needed, because the scalar product of the transition moments has to be divided by the energy differences of the respective states.

The RI-CC2 calculations have been performed with the TURBOMOLE program package[30] and the MP2/6-311+G(d,p) ground-state geometry. Two basis sets were used in these calculations. The first one was the aug-cc-pVDZ basis set.[31,32] In the second case the aug-cc-pVTZ basis set was used on the CCHF olefin group, and the cc-pVDZ basis set was used on all other atoms. From now on the latter basis set will be referred to as TDZ.

The crossing points or local minima on the crossing seam (MXS) were located in two different ways: (i) using the method introduced by Bearpark and co-workers[33] at the SA-2-CAS-(2,2)/6-31G* level of theory as implemented in GAUSSIAN03,[25] (ii) at the multireference configuration interaction with singles and doubles excitations level (MRCI/SA-2-CAS(2,2)/DZ1) by means of the analytic MRCI procedures for energy gradients[34,35] and nonadiabatic derivative coupling vectors[36,37] implemented in the COLUMBUS package.[38,39,40] The DZ1 basis set is composed of the 6-31+G* basis set[41] at the olefin carbon atoms and at the fluorine atom; of the 6-31G** basis set[42] on all other carbon atoms and on the hydrogen atom at the vinyl position; and of the 6-31G basis set[43] on all remaining hydrogen atoms. The ground-state equilibrium geometry and the torsion potential were also computed at the same MRCI level.

3. Results and Discussion

3.1. Vertical Excitations: Valence and Rydberg States. The experimental absorption spectrum of 4MCF, measured by Gedanken et al.,[16] shows two band systems originating at 48 840 cm^{-1} (6.06 eV) and 51 180 cm^{-1} (6.35 eV), which are assigned

TABLE 1: Vertical Excitation Energies (in eV) of (*S*)-(−)-4-Me(C_6H_9)CHF Calculated at the CASSCF/SS-CASPT2/MS-CASPT2 Level of Theory

	SA-2-CAS(2,2)/DZ			SA-2-CAS(2,2)/TZ+d			SA-12-CAS(2,11)/TZ+d							
state	CASSCF	SS-CASPT2	MS-CASPT2	CASSCF	SS-CASPT2	MS-CASPT2	CASSCF	SS-CASPT2	MS-CASPT2	*f*	R^r	R^v	$\langle z^2 \rangle$	exp[j]
1^1A(N)	0.0[a]	0.0[b]	0.0[c]	0.0[d]	0.0[e]	0.0[f]	0.0[g]	0.0[h]	0.0[i]					
2^1A(3s)							4.83	6.30	6.27	0.07	−0.05	−0.06	67.5	6.06
3^1A(*V*)	8.81	6.74	6.75	7.04	5.54	5.56	8.95	6.79	6.50	0.26	0.06	0.10	44.7	6.35 [∼6.5]
4^1A(3pπ)							5.38	6.92	6.94	0.01	0.02	0.03	65.3	
5^1A(3dδ)							5.54	7.05	7.02	0.11	0.02	0.02	85.3	
6^1A(3pπ)							5.22	6.75	7.11	0.05	−0.04	−0.07	93.2	
7^1A(3pσ)							5.88	7.51	7.54	0.00	0.00	0.00	72.6	
8^1A(3dπ)							5.93	7.58	7.60	0.00	0.01	0.01	65.5	
9^1A(3dπ)							5.97	7.63	7.69	0.00	0.00	0.00	113.1	
10^1A(3dσ)							6.41	7.86	7.89	0.01	0.00	0.00	71.3	
11^1A(3dσ)							6.31	7.95	8.00	0.00	0.00	−0.01	86.5	
12^1A(Z)	14.54	12.32	12.36	13.68	12.36	12.38	12.62	12.65	12.68	0.00	0.00	0.00	70.2	

[a] −410.0681 au. [b] −411.36888. [c] −411.36949. [d] −410.0774. [e] −411.54041. [f] −411.54091. [g] −410.0683. [h] −411.64307. [i] −411.64382. [j] Reference 16. Origin of the $\pi\pi^*$ band. The value in brackets is an estimate for the band maximum.

to $\pi \rightarrow$ 3s and the $\pi \rightarrow \pi^*$ (V) transitions, respectively. Unfortunately, band maxima, which could be related to vertical transitions, have not been given in this work for 4MCF. On the basis of the spectrum for the deuterated isotope, the experimental V-state vertical excitation is estimated to lie about 0.2 eV higher in energy than the origin of the band, which leads to a value of ∼6.5 eV.

In Table 1 vertical excitation energies for the states calculated with the CASSCF, single-state SS-CASPT2 and MS-CASPT2 methods are presented. The states are ordered with increasing energy (in eV) according to the MS-CASPT2 results obtained with the (2,11) active space. The character of the states has been assigned after analyzing the configuration-state functions and the molecular orbitals and inspecting the expectation values $\langle x^2 \rangle$, $\langle y^2 \rangle$, and $\langle z^2 \rangle$ of the second Cartesian moments.

The MS-CASPT2 excitation energy for the V state evaluated for the SA-2-CAS(2,2)/DZ reference wave function is overestimated by 0.25 eV with respect to the experimental value (estimated band maximum). Because of the reduced basis set, no mixing with other states, i.e., with Rydberg states, occurs and the state can be assigned to a $\pi \rightarrow \pi^*$ excitation, as manifested in the high weight of the respective configuration-state functions (99%) and also in the eigenvectors of the perturbatively modified wave function. Interestingly, the use of the TZ+d basis set on the same active space, which provides enough flexibility to describe Rydberg states, results in a dramatic (ca. 2 eV) underestimation of the V excitation energy, indicating the presence of intruder states identified as Rydberg excitations (reference weights in all N, V, Z states are about 70%). Any attempt to describe only the valence and the 3s or 3p Rydberg states led to the wrong ordering of the low-lying 3s and V states, as well as strong valence-Rydberg mixings. This leads to the conclusion that the reasonable agreement of the MS-CASPT2/SA-2-CAS(2,2)/DZ results for the V band are the result of a compensation of errors: on one hand the reduced basis set, and on the other the small active space, neglecting electronic correlation.

MS-CASPT2 energies on SA-12-CAS(2,11)/TZ+d wave functions account for several Rydberg states, predicting the 3s state below the *V* state, in excellent agreement with experimental results. As expected, CASSCF energies are strongly overestimated, and it is noticeable that SS-CASPT2 cannot remove completely the mixing. The 1:3 ratio in the oscillator strengths between the 3s and V states is in accord with the intensity of the experimental bands.[16] It is also gratifying to see that the sign of the respective rotatory strengths has been reproduced (3s, (−); V, (+) for (*S*)-(−)-4-Me(C_6H_9)CHF).

TABLE 2: Vertical Excitation Energies (in eV) of (*S*)-(−)-4-Me(C_6H_9)CHF Calculated at the CASPT2 and RI-CC2 Levels (Oscillator Strengths in Parenthesis)

state	RI-CC2 aug-cc-pVDZ	RI-CC2 TDZ	MS-CASPT2 TZ+d	exp[d]
S_0	0.00[a]	0.00[b]	0.00[c]	
S_1 (3s)	6.04	6.21 (0.02)	6.27 (0.07)	6.06
S_5 ($\pi\pi^*$)		6.75 (0.17)	6.50 (0.26)	6.35 [∼6.5]

[a] −411.36175 au. [b] −411.47970. [c] −411.64382. [d] Reference 16. Origin of the $\pi\pi^*$ band. The value in brackets is an estimate for the band maximum.

The RI-CC2 results are shown in Table 2. The energy of the $\pi \rightarrow$ 3s state obtained with both, double- and triple-ζ-quality, basis sets is in good agreement with the experimental result. However, we have not been able to locate the V state at double-ζ level, even when 13 states were calculated. The inclusion of the triple-ζ quality basis-set on the olefin atoms changes drastically this picture. In this case, the V-state energy is 6.75 eV in good agreement with the experimental result.

3.2. Deactivation Paths and Conical Intersections. The similarities between 4MCF, ethylene (C_2H_4) and fluoroethylene (C_2H_3F) will be exploited to gain some insight into the deactivation processes undergone by the photoexcited 4MCF. In the prototype ethylene molecule the first three low-lying excited states are of Rydberg character, whereas at the conical intersection the geometries between the ground and first excited states are purely of valence character, with the Rydberg states higher in energy.[8] Fluoroethylene, the chromophore of 4MCF, in the planar ground-state minimum has the V state embedded in the 3s, 3p Rydberg series, with the 3s state lying below it. The torsion around the CC bond destabilizes the Rydberg states and induces a crossing between the V and the ground states at the twisted geometry (90°), close to which three different MXSs have been located.[14] A similar situation is found for 4MCF, as can be seen in Figure 2a, in which the N and V energies for the rigid torsion τ (see Scheme 1) around the C_1C_2 axis are plotted.

The MS-CASPT2/TZ+d result for $\tau = 0°$ is also shown for comparison. Negative and positive angles correspond respectively to F-eclipsed and F-staggered geometries in relation to the methyl group (cf. Chart 1).

At the MRCI/SA-2-CAS(2,2)/DZ1 level of theory it was not possible to obtain reasonable results for angles $\tau < 45°$ due to valence−Rydberg state mixing. For torsional angles larger than

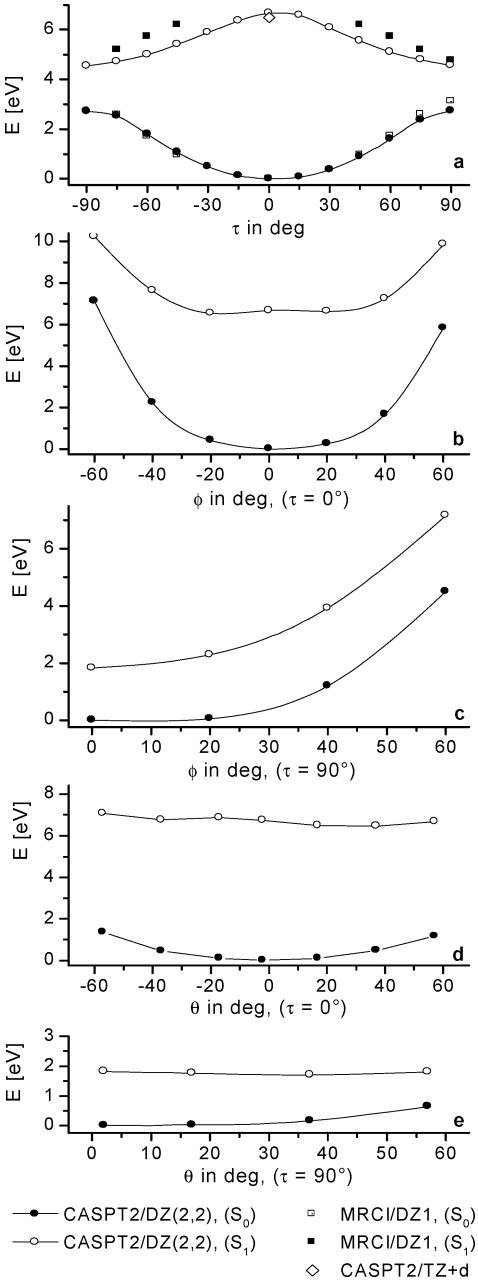

Figure 2. Potential energy profiles along (a) the twisting angle τ, and (b)−(e) pyramidalization degrees of freedom ϕ and θ, for $\tau = 0°$ and $\tau = 90°$. Angles τ and θ are explained in Scheme 1. ϕ is given as the dihedral angle $FC_1C_2C_3$. The electronic ground state and first excited state are shown with filled and open circles, respectively.

SCHEME 1

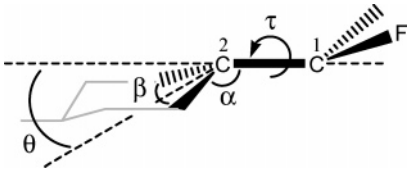

45°, the Rydberg states are energetically higher than the V state, which justifies the use of the CAS(2,2) space and the averaging over two states only. Although the rigid torsion leads to a large reduction in the S_1-S_0 energy gap, it is still 1.65 eV at 90° (1.82 eV at MS-CASPT2/SA-CAS(2,2)/DZ level). Even if a reduced CAS(2,2) reference space may not be enough to fully characterize a conical intersection between the two electronic states,[44] a preliminary search indicates the presence of a

CHART 1

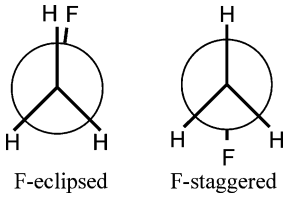

degeneracy point, which was also found in the case of the fluoroethylene.[14] Indeed, the search for conical intersections close to a $\tau = 90°$-twisted geometry reveals that there exists a minimum on the crossing seam in this region. The twisted MXS is characterized in Table 3, Table 4 and Figure 3a. This structure corresponds to the F atom in staggered position with respect to the methyl group (cf. Chart 1). The derivative coupling between S_1 and S_0 (**DC** $= \langle\psi_1|\nabla H\psi_0\rangle$) and gradient difference (**GD** $= (\nabla E_1 - \nabla E_0)/2$) vectors, defining the branching space in which the MXS splits linearly,[9] are also shown in Figure 3a. Similar to the fluoroethylene case, the branching space is mainly composed of the torsional coordinate of the CFH group and by the C_1C_2 stretching coordinate.

The large mass of the fluorine atom implies that the excited-state relaxation path cover regions far from the rigid torsion. Therefore, in analogy with ethylene, it was also interesting to investigate whether the crossing seam extends to pyramidalized structures. Starting from a planar $\tau = 0°$ or a twisted $\tau = 90°$ structure, Figure 2b and 2c show the S_0 and S_1 energy profiles along the pyramidalization angle ϕ, defined as the dihedral angle $C_3C_2C_1F$ (cf. Figure 1), taken as an indicator of the pyramidalization at the CFH group. Although neither the curves in Figure 2b nor those in Figure 2c show intersections, the MXS search starting from $\tau = 90°$ and $\phi = 40°$ (energy gap of ca. 2.72 eV at MS-CASPT2/SA-CAS(2,2)/DZ level of theory) ended it up in a second degeneracy point (Figure 3b). In this MXS, the distances from the hydrogen atom to the two olefin carbon atoms are 1.159 and 1.641 Å, respectively (cf. Table 3). For this reason this degeneracy point has been called H-migration MXS. Intuitively, structures leading to isomerization around a double bond are expected to have longer C═C bond distances, and accordingly in this MXS the C_1C_2 bond distance increases from 1.32 to 1.45 Å. Although the potential energy of this MXS is higher than the energies of the other MXS (see Table 4), it is still accessible with the energy available from the vertical excitation. Different from the twisted MXS, the **DC** and **GD** vectors cannot be described in terms of simple internal coordinates. Nevertheless, it is still apparent that the **DC** vector has a large contribution from the torsional coordinate, and the **GD** is composed of CHF pyramidalization and wagging motions, which favor the H-migration.

Finally, parts d and e of Figure 2 show the potential energy scans along θ, defined as $\cos\theta = -\cos\alpha/\cos\beta/2$ (see Scheme 1), where α and β are the bending angles $C_3C_2C_1$ and $C_4C_2C_3$, respectively (see Figure 1). The angle θ corresponds to geometries pyramidalized at the ethylene C atom that also belongs to the cyclohexane ring, whereas $\tau = 0°$ or 90°, respectively. The smallest energy gap between the S_0 and S_1 states is found for twisted structures (1.47 eV at $\theta = 57°$). The MXS search resulted in a minimum with the fluorine in the eclipsed position characterized in Table 3 and Table 4 (see also Figure 3c) and has been denominated pyramidalized MXS. In passing we note that this MXS can be also found when starting from the twisted MXS where the H and F atoms are exchanged.[45] In this MXS the CC bond is relatively short with a value close to the one found in the ground-state structure (the

TABLE 3: Geometric Parameters (Å and Degrees) for the Ground-State and MXS Geometries of 4MCF and C_2H_3F[a]

	ground state		twisted MXS			H-migration MXS			pyramid. MXS		
	4MCF	C_2H_3F	4MCF MRCI	4MCF CASSCF	C_2H_3F MRCI	4MCF MRCI	4MCF CASSCF	C_2H_3F MRCI	4MF MRCI	4MCF CASSCF	C_2H_3F MRCI
CC	1.320	1.338	1.277	1.260	1.318	1.446	1.447	1.415	1.352	1.357	1.376
CF	1.356	1.357	1.736	1.729	1.378	1.401	1.380	1.357	1.319	1.289	1.327
CH	1.073	1.085	1.073	1.082	1.110	1.159	1.177	1.207	1.099	1.106	1.105
CCF	122.6	121.6	124.6	127.7	125.8	120.8	121.9	122.3	124.4	124.8	122.2
CCH	125.8	126.3	149.3	149.3	133.5	77.2	77.0	72.3	129.5	128.6	132.1
CCX	124.0	121.5	125.5	125.4	143.2	126.8	127.1	119.8	119.0	117.0	107.8
CCY	120.3	118.8	116.6	116.6	94.7	118.5	118.6	119.5	93.7	94.3	107.5

[a] The 4MCF data were obtained at the MRCI/SA-2-CAS(2,2)/DZ1 Level. The data for C_2H_3F were taken from ref 14 and were calculated at the MRCI/SA-3-CAS(2,2)/aug-cc-pVDZ level of theory. X and Y are the carbon atoms in the ring of 4MCF and the H atoms in the CH_2 group of fluoroethylene.

TABLE 4: MXS Energies (eV) of 4MCF and C_2H_3F[a]

	twisted MXS		H-migration MXS		pyramid MXS	
	4MCF	C_2H_3F	4MCF	C_2H_3F	4MCF	C_2H_3F
E(CASSCF)	3.74[b]		3.83[e]		3.05[h]	
E(MRCI)	4.78[c]	4.39	5.24[f]	6.38	4.55[i]	4.10
E(MRCI+Q)	4.71[d]	4.28	5.16[g]	6.11	4.46[j]	3.92

[a] The 4MCF data were obtained at the MRCI/SA-2-CAS(2,2)/DZ1 level. The data for C_2H_3F were taken from ref 14 and were calculated at the MRCI/SA-3-CAS(2,2)/aug-cc-pVDZ level of theory. [b] −409.7681777. [c] −410.49308. [d] −410.65337. [e] −409.7649599. [f] −410.47617. [g] −410.63681. [h] −409.793541. [i] −410.50179. [j] −410.66256.

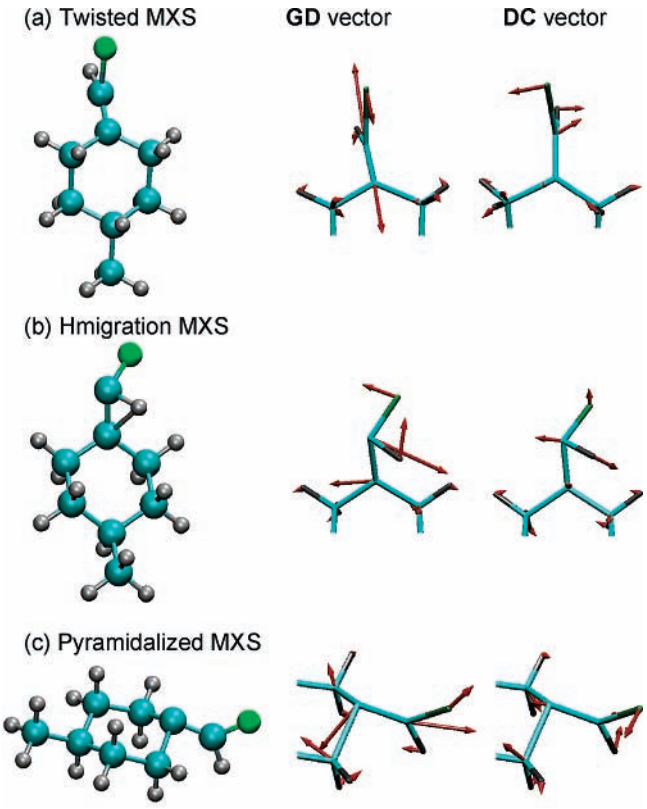

Figure 3. Optimized lowest energy crossing points (MXS) for 4MCF based on MRCI/SA-2-CAS(2,2) wavefunctions and corresponding gradient difference (**GD**) and derivative coupling (**DC**) vectors.

distance C_1C_2 is 1.36 in the MXS vs 1.32 Å in the ground-state minimum). The **DC** and **GD** vectors shown in Figure 3c can be described, as in the twisted MXS, by torsion and C_1C_2 stretching.

Each one of these three degeneracy points can be correlated directly with equivalent structures found in fluoroethylene at a similar level of theory.[14] Table 3 and 4, respectively, show the relevant geometric parameters and the $\pi\pi^*$-state energy for the ground-state and the MXS geometries of 4MCF and C_2H_3F. The excellent correlation between the geometries and energies of the two systems implies that C_2H_3F may be used as a model for investigating the photodynamics of 4MCF, provided that some mechanical constraint is imposed on the motion of the H atoms in the CH_2 group. This could be done, for example, by artificially increasing the isotopic masses of the hydrogen atoms of fluoroethylene that are substituted by the ring in the 4MCF.

After the excitation, the twisted MXS should not be so easily reached as it is in the case of small substituted ethylenes.[46] One reason for that is the already mentioned asymmetry introduced by the large mass of the fluorine atom that implies visiting regions far from rigid torsion relaxation. Another reason is the fact that excitation into the antibonding π^* orbital weakens the CC bond, which will increase during the torsion. However, to reach the twisted MXS, the CC distance must decrease substantially (see Table 3). Thus, several CC periods might be necessary to achieve the required combination of stretching and torsion. Similar effects have been observed in the dynamics of silaethylene.[46] The dynamics of silaethylene and methaniminium cation also have shown that sometimes the relaxation on the excited state can proceed without torsion, by a very early activation of the pyramidalization modes.[46] If this is also true in the case of 4MCF, the regions of the crossing seam involving pyramidalization can be particularly important for the deactivation process.

4. Conclusions and Outlook

A detailed characterization of the electronically excited states involved in the UV absorption spectrum of the chiral (4-methylcyclohexylidene) fluoromethane (4MCF) has been provided at different levels of theory. Using multiconfigurational multistate CASPT2 on CASSCF wavefunctions and coupled-cluster methods (RI-CC2) a Rydberg 3s state is predicted below the valence $\pi\pi^*$ state. The calculated vertical energies of the 3s and valence states, their oscillator strength ratio, and their rotatory strengths are in good agreement with the experimental results reported by Gedanken et al.[16]

In analogy with ethylene and more specifically with fluoroethylene, potential energy profiles along the double bond torsion and pyramidalization of each carbon have been constructed. Such energy profiles give some indication about the localization of the degeneracy points, which have been further optimized. These curves also show that these particular internal coordinates alone are not enough to describe the isomerization process, because the minimum energy gap along them is still too large if geometry relaxation is not taken into account. Explicitly, three degeneracy points involving the torsional and pyramidalization coordinates have been located and all of them can be directly

correlated with equivalent crossing points in fluoroethylene. Such conical intersections will be further analyzed using elementary reaction coordinates and the geometrical phase effect.[47]

On the basis of our experience with the photodynamics of substituted ethylenes,[46] we have discussed how the relaxation of 4MCF should proceed through some far-from-rigid torsional motion. At the present stage of knowledge it is not possible to anticipate which region of the crossing seam is the most important for the deactivation process, if any. Dynamics simulations on fluoroethylene are in progress and it should shed some light on this issue.

Acknowledgment. We thank Y. Haas for fruitful discussions about conical intersections. Financial support from the DFG within the trilateral project Germany-Israel-Palestine Ma 515/22-1 is gratefully acknowledged. L.G. thanks the "Berliner Programm zur Förder ung der Chancengleichheit für Frauen in Forschung und Lehre". M.B. and H.L. acknowledge the support by the Austrian Science Fund within the framework of the Special Research Program F16 (Advanced Light Sources) and Project P18411-N19.

Supporting Information Available: MXS of 4MCF and Cartesian coordinates. This material is available free of charge via the Internet at http://pubs.acs.org.

References and Notes

(1) Feringa, B., Ed. *Molecular Switches*; Wiley-VCH: New York, 2003.

(2) Balzani, V., Credi, A., Venturi, M., Eds. *Molecular Devices and Machines*; Wiley-VCH: New York, 2004.

(3) Crick, F. *Life Itself*; McDonald & Co.: London, 1981.

(4) See, e.g.: Feringa, B.; Van Delden, R. A.; Koumura, N.; Geertsema, E. M. *Chem. Rev.* **2000**, *100*, 1789.

(5) Kneip, C.; Hildebrandt, P.; Schlamann, W.; Braslavsky, S. E.; Mark, F.; Schaffner, K. *Biochemistry* **1999**, *38*, 15185.

(6) See for instance: (a) Ben-Nun, M.; Molnar, F.; Lu, H.; Phillips, J. C.; Martínez, T. J.; Schulten, K. *Faraday Discuss.* **1998**, *110*, 447. (b) Schreiber, M.; Sugihara, M.; Okada, T.; Buss, V. *Angew. Chem., Int. Ed.* **2006**, *45*, 4274.

(7) Ko, C.; Levine, B.; Toniolo, A.; Manohar, L.; Olsen, S.; Werner, H.-J.; Martínez, T. J. *J. Am. Chem. Soc.* **2003**, *125*, 12710.

(8) See exemplarily: (a) Serrano-Andrés, L.; Merchán, M.; Nebot-Gil, I.; Lindh, R.; Roos, B. O. *J. Chem. Phys.* **1993**, *98*, 3151. (b) Ben-Nun, M.; Martínez, T. *J. Chem. Phys. Lett.* **1998**, *298*, 57. (c) Barbatti, M.; Paier, J.; Lischka, H. *J. Chem. Phys.* **2004**, *121*, 11614. (d) Krawczyk, R. P.; Viel, A.; Manthe, U.; Domcke, W. *J. Chem. Phys.* **2003**, *119*, 1397. (e) Baeck, K. K.; Martínez, T. J. *Chem. Phys. Lett.* **2003**, *375*, 299. (f) Quenneville, J.; Martínez, T. J. *J. Phys. Chem.* **2003**, *107*, 829. (g) Viel, A.; Krawczyk, R. P.; Manthe, U.; Domcke, W. *J. Chem. Phys.* **2004**, *120*, 11000.

(9) *Advanced Series in Physical Chemistry: Conical Intersections*; Domcke, W., Yarkony, D. R., Köppel, H., Eds.; World Scientific Publishing Co. Pte. Ltd.: Singapore, 2004; Vol. 15.

(10) (a) Mulliken, R. S. *J. Chem. Phys.* **1977**, *66*, 2448. (b) Wilkinson, P. G. *Can. J. Phys.* **1956**, *34*, 643. (c) Wilden, D. G.; Comer, J. *J. Phys. B* **1980**, *13*, 1009. (d) McDiarmid, R. *J. Phys. Chem.* **1980**, *84*, 64. (e) Merer, A. J.; Mulliken, R. S. *Chem. Rev.* **1969**, *69*, 639. (f) Gedanken, A.; Kuebler, N. A.; Robin, M. B. *J. Chem. Phys.* **1982**, *76*, 46. (g) Williams, A.; Cool, T. A. *J. Chem. Phys.* **1991**, *94*, 6358. (h) Johnson, E.; Johnston, D. B.; Libsky, S. *J. Chem. Phys.* **1979**, *70*, 3844. (i) van Veen, E. H. *Chem. Phys. Lett.* **1976**, *41*, 540. (j) Snyder, P. A.; Schatz, P. N.; Rowe, E. W. *Chem. Phys. Lett.* **1984**, *110*, 508.

(11) Belanger, G.; Sandorfy, C. *J. Chem. Phys.* **1971**, *55*, 2055.

(12) Ben-Nun, M.; Martínez, T. *Chem. Phys.* **2000**, *259*, 237.

(13) Quenneville, J.; Martínez, T. J. *J. Phys. Chem. A* **2003**, *107*, 829.

(14) Barbatti, M.; Aquino, A. J. A.; Lischka, H. *J. Phys. Chem. A* **2005**, *109*, 5168.

(15) Arulmozhiraja, S.; Fukuda, R.; Ehara, M.; Nakatsuji, H. *J. Chem. Phys.* **2006**, *124*, 034312.

(16) Gedanken, M. D.; Huang, J.; Rachon, J.; Walborsky, H. M. *J. Am. Chem. Soc.* **1988**, *110*, 4593.

(17) Kröner, D.; González, L. *Phys. Chem. Chem. Phys.* **2003**, *5*, 3933.

(18) Handy, N. C.; Tozer, D. J. *J. Comput. Chem.* **1999**, *20*, 106.

(19) Fujimura, Y.; González, L.; Kröner, D.; Manz, J.; Mehdaoui, I.; Schmidt, B. *Chem. Phys. Lett.* **2004**, *386*, 248.

(20) (a) Hoki, K.; Sato, M.; Yamaki, M.; Sahnoun, R.; González, L.; Koseki, S.; Fujimura, Y. *J. Phys. Chem. B* **2004**, *108*, 4916. (b) Hoki, K.; González, L.; Shibl, M. F.; Fujimura, Y. *J. Phys. Chem. A* **2004**, *108*, 6455.

(21) (a) Roos, B. O.; Taylor, P. R.; Siegbahn, P. E. M. *Chem. Phys.* **1980**, *48*, 157. (b) Roos, B. O. *Int. J. Quantum Chem.* **1980**, *14*, 175.

(22) Finley, J.; Malmqvist, P. A.; Roos, B. O.; Serrano-Andrés, L. *Chem. Phys. Lett.* **1998**, *288*, 299.

(23) Köhn, A.; Hättig, C. *J. Chem. Phys.* **2003**, *119*, 5021.

(24) Hättig, C. *J. Chem. Phys.* **2003**, *118*, 7751.

(25) Frisch, M. J.; Trucks, G. W.; Schlegel, H. B.; Scuseria, G. E.; Robb, M. A.; Cheeseman, J. R.; Montgomery, J. A., Jr.; Vreven, T.; Kudin, K. N.; Burant, J. C.; Millam, J. M.; Iyengar, S. S.; Tomasi, J.; Barone, V.; Mennucci, B.; Cossi, M.; Scalmani, G.; Rega, N.; Petersson, G. A.; Nakatsuji, H.; Hada, M.; Ehara, M.; Toyota, K.; Fukuda, R.; Hasegawa, J.; Ishida, M.; Nakajima, T.; Honda, Y.; Kitao, O.; Nakai, H.; Klene, M.; Li, X.; Knox, J. E.; Hratchian, H. P.; Cross, J. B.; Bakken, V.; Adamo, C.; Jaramillo, J.; Gomperts, R.; Stratmann, R. E.; Yazyev, O.; Austin, A. J.; Cammi, R.; Pomelli, C.; Ochterski, J. W.; Ayala, P. Y.; Morokuma, K.; Voth, G. A.; Salvador, P.; Dannenberg, J. J.; Zakrzewski, V. G.; Dapprich, S.; Daniels, A. D.; Strain, M. C.; Farkas, O.; Malick, D. K.; Rabuck, A. D.; Raghavachari, K.; Foresman, J. B.; Ortiz, J. V.; Cui, Q.; Baboul, A. G.; Clifford, S.; Cioslowski, J.; Stefanov, B. B.; Liu, G.; Liashenko, A.; Piskorz, P.; Komaromi, I.; Martin, R. L.; Fox, D. J.; Keith, T.; Al-Laham, M. A.; Peng, C. Y.; Nanayakkara, A.; Challacombe, M.; Gill, P. M. W.; Johnson, B.; Chen, W.; Wong, M. W.; Gonzalez, C.; Pople, J. A. *Gaussian 03*, revision C.02; Gaussian, Inc.: Wallingford, CT, 2004.

(26) Kaufman, K.; Baumeister, W.; Jungen, M. *J. Phys. B − At. Mol. Opt. Phys.* **1989**, *22*, 2223.

(27) Malmqvist, P. A.; Rendell, A.; Roos, B. O. *J. Phys. Chem.* **1990**, *94*, 5477.

(28) Roos, B. O.; Andersson, K. *Chem. Phys. Lett.* **1995**, *245*, 215.

(29) Karlström, G.; Lindh, R.; Malmqvist, P. A.; Roos, B. O.; Ryde, U.; Veryazov, V.; Widmark, P.-O.; Cossi, M.; Schimmelpfennig, B.; Neogrady, P.; Seijo, L. *Comput. Mater. Sci.* **2003**, *28*, 222.

(30) Ahlrichs, R.; Bär, M.; Häser, M.; Horn, H.; Kölmel, C. *Chem. Phys. Lett.* **1989**, *162*, 165.

(31) Dunning, T. H., Jr. *J. Chem. Phys.* **1989**, *90*, 1007.

(32) Kendall, R. A.; Dunning, T. H., Jr.; Harrison, R. J. *J. Chem. Phys.* **1992**, *96*, 6769.

(33) Bearpark, M. J.; Robb, M. A.; Schlegel, H. B. *Chem. Phys. Lett.* **1994**, *223*, 269.

(34) Shepard, R.; Lischka, H.; Szalay, P. G.; Kovar, T.; Ernzerhof, M. *J. Chem. Phys.* **1992**, *96*, 2085.

(35) Lischka, H.; Dallos, M.; Shepard, R. *Mol. Phys.* **2002**, *100*, 1647.

(36) Lischka, H.; Dallos, M.; Szalay, P. G.; Yarkony, D. R.; Shepard, R. *J. Chem. Phys.* **2004**, *120*, 7322.

(37) Dallos, M.; Lischka, H.; Shepard, R.; Yarkony, D. R.; Szalay, P. G. *J. Chem. Phys.* **2004**, *120*, 7330.

(38) Lischka, H.; Shepard, R.; Brown, F. B.; Shavitt, I. *Int. J. Quantum Chem.* **1981**, *S15*, 91.

(39) Lischka, H.; Shepard, R.; Shavitt, I.; Pitzer, R. M.; Dallos, M.; Mueller, Th.; Szalay, P. G.; Brown, F. B.; Ahlrichs, R.; Boehm, H. J.; Chang, A.; Comeau, D. C.; Gdanitz, R.; Dachsel, H.; Ehrhardt, C.; Ernzerhof, M.; Hoechtl, P.; Irle, S.; Kedziora, G.; Kovar, T.; Parasuk, V.; Pepper, M. J. M.; Scharf, P.; Schiffer, H.; Schindler, M.; Schueler, M.; Seth, M.; Stahlberg, E. A.; Zhao, J.-G.; Yabushita, S.; Zhang, Z.; Barbatti, M.; Matsika, S.; Schuurmann, M.; Yarkony, D. R.; Brozell, S. R.; Beck, E. V.; Blaudeau, J.-P. *COLUMBUS, an ab initio electronic structure program, release 6.0*, 2006.

(40) Lischka, H.; Shepard, R.; Pitzer, R. M.; Shavitt, I.; Dallos, M.; Müller, Th.; Szalay, P. G.; Seth, M.; Kedziora, G. S.; Yabushita, S.; Zhang, Z. *Phys. Chem. Chem. Phys.* **2001**, *3*, 664.

(41) Clark, T.; Chandrasekhar, J.; Spitznagel, G. W.; Schleyer, P. V. R. *J. Comp. Chem.* **1983**, *4*, 294.

(42) Hariharan, P. C.; Pople, J. A. *Theor. Chim. Acta* **1973**, *28*, 213.

(43) Hehre, W. J.; Ditchfield, R.; Pople, J. A. *J. Chem. Phys.* **1972**, *56*, 2257.

(44) Zilberg, S.; Haas, Y. *Photochem. Photobiol. Sci.* **2003**, *2*, 1256.

(45) If one starts from the twisted MXS (Figure 3a), with the H and F atoms exchanged, but an opposed CHF angle, another pyramidalized MXS with the F-eclipsed can be found. This new structure is electronically equivalent to Figure 3c, but with the C═C bond making a positive angle with the CCC plane of the ring, whereas the structure 3a makes a negative angle. The coordinates and energies of this new MXS are given in the Supporting Information.

(46) (a) Barbatti, M.; Aquino, A. J. A.; Lischka, H. *Mol. Phys.* **2006**, *104*, 1053. (b) Zechmann, G.; Barbatti, M.; Lischka, H.; Pittner, J.; Bonačiać-Koutecký, V. *Chem. Phys. Lett.* **2006**, *418*, 377.

(47) Haas, Y.; Cogan, S.; Zilberg, S. *Int. J. Quantum Chem.* **2005**, *102*, 961.